Error Compensation in Distance Relays Caused by Wind Power Plants in the Power Grid

L. A. Trujillo G.*, A. Conde E and Z. Leonowicz

Universidad Autónoma de Nuevo León, UANL, FIME, Av. Universidad S/N Ciudad Universitaria, San Nicolás de los Garza, N.L, C.P. 66451, México

Wroclaw University of Technology, Faculty of Electrical Engineering, Wyb. Wyspianskiego 27, 50-370 Wroclaw, Poland

* Corresponding author. Tel.: +52 81 11002384.

E-mail address: luistrujillo84@gmail.com (L. Trujillo), con_de@yahoo.com (A. Conde), leonowicz@ieee.org (Z. Leonowicz)

***Abstract*-- This article presents the Prony method as a filtering technique for distance relays. First, the effect of non-filtered frequency components generated by Wind Power Plants in distance relays is evaluated in a simplified model of a doubly fed induction generator, resulting in an error of apparent impedance measurement. Then, the effects of non-filtered frequency components for typical distance relay are presented. The error in apparent impedance measurement is evaluated in reach and operation time of the relay; a distorted characteristic of the mho distance relay is shown in the impedance plane. Finally, Prony method as a filtering technique is implemented as a solution of the apparent impedance measurement error, and the simulated case and a real fault event are evaluated to validate the proposed distance relay algorithm. Thus the asynchronous frequency components of voltage and current signals are identified and filtered, as a result the performance of the distance relay is enhanced.**

***Keywords*-- wind power plant; Prony method; distance relay; protective relays.**

1. Introduction

Nowadays, the technological advancement of alternative sources of renewable energy, such as wind power generation plants which have commonly been used to supply power to a determined load block as a distributed generation, has allowed interconnection with the electric power system. This has helped to reduce CO2 emissions due to the fossil fuel needs of electric generation power plants [1]. The main problem with wind power plants grid connection is that the wind is not constant and, consequently, the generated power is not constant. This generates fluctuations in voltage and frequency. Fluctuations have been minimized by different schemes of operation, like the doubly fed induction generator scheme (DFIG) that uses a back-to-back power converter to control the active and reactive power generated by the wind turbine [2]. The grid connection of a wind power plant affects the electric power system variables, for example: voltage, load current, frequency, power generated and power system transients induced by the switching of capacitor banks [6,7].

Performance studies of protection systems must be made to evaluate the impact of wind power plants in protective relays [2-5]. The protective relays of the grid have constant pickup values and due to the dynamic behavior of a wind power plant as seen by the distance relay as an infeed, the performance of the protection system could be compromised. This affects the distance relay operation, which causes an overreach/underreach [8-11].

Also, some frequency components as inter-harmonics and sub-harmonics generated by the wind power plant [6] are not filtered by the distance relays and this causes problems in fault detection [12]. The main focus of the analysis presented in this paper is to obtain a better estimate of fundamental frequency phasors of voltage and current signals required by distance relays, because due to non-filtered frequency components, the conventional digital filters generate an error in the fundamental frequency phasor estimation, and by consequence a fault detection problem. The Prony method results in a good alternative to get a correct apparent impedance measurement by estimating the fundamental frequency phasor of voltage and current require by the distance relay [7]. A model of a Wind Power Plant is presented to perform transmission line protection analysis, so the conventional filter and proposed filter using Prony method could be evaluated. The DFIG scheme and the mho characteristic are studied in this paper because are the most common in the power systems; however another wind power models and other distance relay characteristic can be used with the same methodology.

2. MODEL SIMPLIFICATION OF DFIG FOR PROTECTION SYSTEM ANALYSIS

This section describes the model of the DFIG discrete detailed model scheme [1] and an evaluation of the model for protection systems analysis. To perform fault analysis in transmission systems, it is not practical to represent all wind turbines individually in a wind power plant. It should be represented as a single equivalent turbine equal to the sum of each one of the turbines in series with a reactance that represents the equivalent impedance of each turbine transformer, power cables, etc. In this particular case a DFIG scheme model is presented to perform the protection system analysis. The control loops and elements that show slow response times in the DFIG scheme when compared with the distance relay response times are considered as constants. This is due to the fact that in a fault condition in the power grid these elements will not impact on the distance relay operation. This simplified model is evaluated in a power system simulation in the following subsections.

In accordance with the time response of each block of DFIG detailed model scheme, a reduction of the system has been made according to the considerations recommended in [13]. In the pitch angle controller, the time response of a change in speed to compensate for the wind speed up or speed down to optimize the turbine speed is in the range of 1-3Hz (20 cycles of fundamental frequency) due to the size and weight of the blades, so the pitch angle is considered as a constant. In the rotor speed controller, the time response of a change in wind speed is in the range of 20 Hz. It should be mentioned that a change in wind speed causes a change of rotor speed and during a grid fault the rotor speed controller will not respond. Therefore, the time response of the speed control is not considered due to the time of fault detection of distance relays algorithm is 1-2 cycles.

The voltage terminal controller in DFIG detailed model represents the reactive power capacity of the wind power plant during a voltage dip, or an external fault in the power system, although not every wind power plant has this configuration. For example, in Germany and Spain their grid codes for interconnecting wind power plants to the power system specify that the wind power plants should have reactive power compensation of 100% of capacity of the wind power plant during an external fault in the power system [14]. It should be mentioned that during an external fault the time response of the reactive power compensation control is about 15 cycles [15], and the reactive power compensation will not affect the operation of the distance relay due to the slow time response when it is compared to the distance relay response to the fault.

In Fig. 1 the model scheme for the DFIG for protection system analysis is presented. The pitch angle β; the wind speed Vw; the mechanical power generated by the wind Pm; and the active and reactive power references required by the power converter Pset and Qset are considered constants. This is due to the dynamic responses of these variables being too slow in comparison with the response time of the distance relays.

2.1 Test system

In this section, a test system is shown in Fig. 2 to evaluate the distance relay operation using Matlab/Simulink. The system consists of a wind power plant with DFIG discrete model scheme represented as a single equivalent turbine interconnected to a 60Hz power system, with a two-phase fault applied at 80% in the transmission line [16]. The response of the wind power plant during an external fault is evaluated in the impedance plane by the measurement of voltage and current signals in the bus B of the test system. By using these signals as the input signals in the distance relay algorithm the apparent impedance measurement can be evaluated.

The system parameters for the test system for the evaluation of the detailed and simplified model are shown in Table 1.

2.2 Measured Signals

The voltage and current signals measured at bus B of the test system are shown in Fig. 3 for the wind power plant proposed model, the sampling rate of the signals is 32 samples per cycle. A two phase to ground fault is applied in the transmission line at 0.03s over a duration of 100 ms. The two phase to ground fault is analyzed due to the fact that is nonsymmetrical and has a major impact in the response of the power converter [1].

As shown in Fig. 4, the error in the simplified and detailed model is of low magnitude. The difference between the simplified and detailed model is shown in Fig. 4. The percentage error of Z estimate using the phasor estimates of one cycle window length of voltage and current signals in Bus B of the simplified and detailed model is presented in Fig. 5 where the average percentage error is 0.5%.

2.3 Impedance Plane

The frequency spectrum of voltage and current signals (Fig. 3 and Fig. 4) is calculated during the fault period. The frequency components detected during the fault are shown in Table 2 and 3 for the detailed and simplified model respectively, it can be seen that low frequency components (sub-harmonics) and inter-harmonics have been detected. The frequency spectra of the signals using the detailed and simplified model are shown in Fig. 6.

The apparent impedance measured by the relay at bus B is shown in Fig. 7 and it can be seen that during the fault period an error in the impedance estimation appears. For comparison, the simplified model and the detailed model have been used, it can be seen that the simplified model for protection system analysis is appropriate, since the control systems time response (considered as constants in the simplified model) of a DFIG scheme are too slow in comparison with the time response of the fault detection of the distance relay. Using the simplified model, it is possible to analyze the operational dynamics of protection relays when wind power plants with the DFIG scheme are interconnected with the power grid.

3. Distance Relay Model

The performance evaluation of a distance relay is dependent on its ability to detect faults within its zone of protection. The distance relay detects a fault condition when the system impedance reaches the tripping characteristic, but the decision to trigger must be considered because there are phenomena, such as power oscillations, that can cause penetration of the characteristic and that are not the result of a fault condition.

The distance relay operation is based on the phase comparison of two input signals, operation and polarization, to determine the trip condition, and this is performed by having signals sampling time, input analog filter, digital filter, and trip output signal [17], all of these conventional distance relay stages will be discussed in this section.

The distance relay models have a phase comparator that responds to the phase angle displacement between input signals [18]. The input signals of phase comparator are obtained using the electric signals measured by the instrument transformers and design constants. The model of the distance relay is shown in (1).

$$\begin{aligned} S_1 &= \overline{k}_1 \cdot \overline{V}_r + \overline{Z}_{R1} \cdot \overline{I}_r \\ S_2 &= \overline{k}_2 \cdot \overline{V}_r + \overline{Z}_{R2} \cdot \overline{I_r} \end{aligned} \tag{1}$$

where S_1 and S_2 are the input signals to establish the trip signal; $\bar{k}_1$ and $\bar{k}_2$ are the constants for the design; $\bar{Z}_{R1}$ is the replica impedance of the protected transmission line; and $\bar{Z}_{R2}$ is the impedance multiplied by the current, resulting in a polarization voltage; $\bar{I}_r$ and $\bar{V}_r$ are the electric input signals which are estimated by the phasor estimation technique to obtain the fundamental frequency phasor [15].

The phase relays are required for the detection of phase to phase faults, an important aspect in the distance relay design is that the correct values of $\bar{I}_r$ and $\bar{V}_r$ has to be selected, the electric input signals that correspond to phase distance relay unit (BC) for voltage is V_{bn}-V_{cn} and for current is I_b-I_c and the typical sampling time used is 16-32 samples per cycle for 60 Hz[17,19].

In Fig. 8 the Mho operation characteristic is presented in a two dimensional and tridimensional space of the impedance plane through time, the time is represented by the one cycle window length displacement. The estimated fundamental phasors of voltage and current are used for the relay (phase relay unit). The input signals Vr and Ir are used to form the operation characteristic and the phase comparator scheme, in this paper the Mho characteristic is evaluated.

The algorithm of the relay should take the voltage and current phasors as input to determine the operating condition. These input signals must be filtered, because they may include electrical phenomena that exhibit a random characteristic, which makes it impossible to determine the fault location. Digital processing should be used to eliminate unwanted quantities such as the direct current component, transients from instrument transformers, traveling wave reflections, and other interference signals. Relay operation should be established using only the fundamental signal components at the nominal frequency because these are proportionately affected by the fault location.

The fundamental phasors of current and voltage can be calculated with two filter stages analog and digital (see Fig. 9). Generally the analog filter used is a Butterworth filter of 2nd or 4th order with a cut-off frequency of 360 Hz (see Fig. 10), this filter is preferred because it has flat response in passband and decreasing monotonically in stopband [20].

After the analog filter stage there is the process of digitalization of the analog signal, the increment in the sampling frequency allows a substantial increment in the signal resolution, but the microprocessor burden is increased. The “aliasing” effect reduction is obtained by tuning between analog and digital filter allowing an overlap of the filter frequencies, it is possible to remove analog filter by oversampling the signal.

The digital filtering is performed with FIR (Finite Impulse Response) filters, because there is no recursion, i.e. the output depends only from the input and not from past values of the output, the memory of the previous conditions of the signal does not have a benefit in obtaining the fault condition by the distance relay. Also, the IIR (Infinite Impulse Response) filter produces in general a phase angle distortion, opposite to FIR filters. This condition allows that their frequency response has natural zeros in the harmonic frequencies allowing a rejection of these frequency components (see Fig. 10).

The distance relay algorithms used for the fundamental frequency component estimation of voltage and current signals use the Fourier or Cosine filter (see Fig. 10). In studies performed for the evaluation of digital filters [12] for the estimation of the fundamental component the Cosine filter presented good results in the rejection of the DC component during the fault period [12].

The distance relay model is based in the fundamental frequency phasor (Eq. 1), but due to the digital filters used in distance relays errors in the fundamental frequency phasor estimate are present due to the existence of interharmonics and/or subharmonics in the voltage and current signals during the fault period. When these frequency components are present, the digital filter generates an error in the fundamental frequency phasors estimates of voltage and current. The distance relay model needs an estimate of the fundamental frequency phasors of voltage and current during the fault period, so an estimate of the apparent impedance can be calculated by the relay, but with the increment of power electronics equipment or compensation used to have a more dependable transmission system this type of equipment generate frequency components that the common digital filters as Fourier and Cosine cannot reject.

A characterization of the problem using the distance relay model in (1) its represented in (2) as follows:

$$
\begin{aligned}
S_1 &= k_1\angle\alpha_1\left[V_{h1}e^{j\theta_{Vh1}} + \overbrace{\sum V_i e^{j\theta_{Vi}} + \sum V_s e^{j\theta_{Vs}}}^{\text{Error in estimation}}\right] + Z_{R1}\angle\theta_1\left[I_{h1}e^{j\theta_{Ih1}} + \overbrace{\sum I_i e^{j\theta_{Ii}} + \sum I_s e^{j\theta_{Is}}}^{\text{Error in estimation}}\right] \\
S_2 &= k_2\angle\alpha_2\left[V_{h1}e^{j\theta_{Vh1}} + \sum V_i e^{j\theta_{Vi}} + \sum V_s e^{j\theta_{Vs}}\right] + Z_{R2}\angle\theta_2\left[I_{h1}e^{j\theta_{Ih1}} + \sum I_i e^{j\theta_{Ii}} + \sum I_s e^{j\theta_{Is}}\right]
\end{aligned} \qquad (2)
$$

where h1=fundamental frequency; i=interharmonics, i>1; s=subharmonics, s<1. The graphical representation of the error in the estimate is presented in Fig. 11, when this kind of frequency components are present in the voltage and current signals an error in the fundamental frequency phasors of voltage and current will cause an error in the operation characteristic, the operation characteristic is formed by the comparison signals in (1), and at the same time require the voltage and current phasors, so from (2) the resultant operation characteristic is formed (see Fig. 11).

The operation scheme for a distance relay is shown in Fig. 12, where the first step is to define the operational characteristic, selecting the design constants and the settings of the distance relay. This process is made off-line and is defined by the manufacturer of the relay. In the next step, the electric input signals measured on-line from the instrument transformers (voltage and current) are used to estimate the fundamental phasor component, see Fig. 12 on-line process, the new algorithm is focused in using a different digital filtering technique for the estimation of fundamental phasor component. With the fundamental phasor component estimated, the comparison signals are formed and the trip condition is evaluated. The trip condition criterion is then performed to generate a trip signal.

4. Distance relay algorithm using Prony method as a filtering technique

In this section the proposed distance relay algorithm using Prony method is presented. The Prony method has been studied as a power quality analysis tool [21, 22, 23] obtaining good results in comparison with FFT, also it has been used in power system stability studies [24]. The proposed algorithm for distance relay using Prony method estimates the signals parameters (amplitude, frequency, phase angle and damping factors) using one cycle window of data, so the real fundamental frequency of the voltage and current signals can be extracted during the first fault period and that the error in the phasor estimates (see section 3) could be reduced.

The Prony method is a signal processing technique based on signal estimation [21,22, 23] where a signal *y(t)* is considered and its samples [*y(1) y(2)…y(n)*] are obtained using a sampling frequency f_s. The Prony model approximates the sampled data with the following linear combination of *N* complex exponentials:

$$y(t) = \sum_{n=1}^{N} A_n e^{\sigma_n t} \cos\left(2\pi f_n t + \theta_n\right) \quad (3)$$

$$y_M = \sum_{n=1}^{N} B_n \lambda_n{}^M \quad (4)$$

The signal *y(t)* in (3) has four elements: Magnitude A_n, damping factor σ_n, frequency f_n, and the phase angle θ_n.. Each exponential term with different frequency is a unique signal mode of the original signal *y(t)*. So, using the Euler theorem and total time *t=MT*, where *M* is the length of the signal and *T* is the time between samples, equation (3) can be rewritten as (4). From (4) the parameters of the signal *y(t)* can be found as it is mentioned in the

Prony method literature [21,22,23].

So that Prony method can be implemented in distance relay algorithms is necessary to obtain the order *N* of the linear prediction model (LPM). The order is obtained evaluating the mean square error (MSE) for one cycle window of data of N=1,2...Ns, where Ns is the samples per cycle in a window data. The MSE for each value of *N* is calculated and the MSE of lesser magnitude is selected for the corresponding *N* value, so this value of *N* is the optimum estimate of the model signal parameters. The proposed distance relay algorithm is shown in Fig. 13, and is intended to estimate the real signal parameters during the first fault period.

In Fig. 14 the Prony phasor magnitude of estimated fundamental phasors and the phase angle estimated with Prony are calculated and the compensated phasors are formed, the compensated phasors are used as the fundamental phasors in the distance relay model to enhance the reach.

4.1 Formulation

The formulation of the proposed distance relay algorithm using the Prony estimated phasors is presented as follows:

$$\begin{aligned} S_1 &= k_1\angle\alpha_1\overbrace{\left[V_{P1}e^{j\theta_{V_{P1}}}\right]}^{\text{Prony phasor estimation}} + Z_{R1}\angle\theta_1\overbrace{\left[I_{P1}e^{j\theta_{I_{P1}}}\right]}^{\text{Prony phasor estimation}} \\ S_2 &= k_2\angle\alpha_2\left[V_{P1}e^{j\theta_{V_{P1}}}\right] + Z_{R2}\angle\theta_2\left[I_{P1}e^{j\theta_{I_{P1}}}\right] \end{aligned} \quad (5)$$

where P1 is the fundamental component estimated with Prony. For the analysis of the proposed algorithm the Mho characteristic will be evaluated. The distance relay model for a Mho characteristic is:

$$\begin{aligned} S_1 &= k_1\angle\alpha_1\left[V_{P1}e^{j\theta_{V_{P1}}}\right] + Z_{R1}\angle\theta_1\left[I_{P1}e^{j\theta_{I_{P1}}}\right] \\ S_2 &= k_2\angle\alpha_2\left[V_{P1}e^{j\theta_{V_{P1}}}\right] \end{aligned} \quad (6)$$

where $k_1=k_2=1, \alpha_1=180^o, \alpha_2=0^o$ and $Z_{R2}\angle\theta_2=0$ in (5) for a Mho characteristic, so the distance relay model for the Mho characteristic is as shown in (6).

5. Analysis of proposed distance relay algorithm

The proposed algorithm presented in section 4 is validated using voltage and current signals of the simulated case using the simplified model in section 2 and using signals from a real fault event, it should be mentioned that a phase distance relay unit (BC) is evaluated with a pickup value of protection zone 1 of 80% of the line impedance and that a down sampling to 16 samples per cycle of the signals is performed.

5.1 Simulated Case

The simulated case data is presented in section 2 and the voltage and current signals used for the analysis are from Fig. 8. Again we use 60 Hz signals, for this test 65.92 _73.7° ohms is considered for the setting of distance relay (80% of the line). In Fig. 15 the Mho characteristic is presented in a tridimensional space of the impedance plane using the voltage and current signals (V_r and I_r) of Fig. 9. A reach error of the relay due to the frequency components (sub-harmonics and inter-harmonics) can be observed in Fig. 15b, the reach error percentage is calculated using the Cosine conventional digital filter to obtain the tridimensional estimated mho operation characteristic, then the reach error is calculated using the pickup value of zone 1 and the reach value obtained from the tridimensional operation characteristic during the first one cycle window data with fault values only.

The reach error during the first fault period (first one cycle window data with fault values only) of the distance relay is 5.7% (maximum deviation of Fig. 16b compared with the characteristic of Fig. 8) in the test system of Fig. 2. In contrast the reach error using the proposed algorithm is 0.02% (Fig. 16). The operation time (fault detection) using the Cosine filter could not generate a trip signal, so the fault could not be detected. The operation time of proposed algorithm is 0.75 cycles, so the fault is detected. The results confirm that the use of the proposed distance relay algorithm a reach error reduction in the relay is obtained and in consequence a reduction in the operation time.

The operation characteristic allows to evaluate the reach error in the distance relay. In addition the fault impedance trajectory in the impedance plane allows to evaluate the operation time of the relay. Then the error measurement due to asynchronous frequency components affects the reach and the operation time of the distance relay.

5.2 Real fault event

The real fault event corresponds to a 230kV transmission line with an impedance of 75/_82.4^{o} ohms, the transmission line is interconnected with La Venta II wind power plant in Oaxaca, México with an approximate 100 MW generation capability. The power system frequency is 60 Hz, and the sampling frequency of the recorded signals is 128 samples per cycle (see Fig. 17). There is no record of operation of protection relays, so this analysis only focuses on the reach error caused by the unfiltered frequency components.

The distance relay characteristic was defined for the real event, the voltage and current signals were filtered using Cosine filter, then the characteristic was formed using (1) and the design constants in Fig. 8. For the improved method, the real event signals were filtered using the Prony method as described in Fig. 13 thus, the same process is used for the proposed method, and then (6) is used with the Mho design constants. The relay characteristic results in Fig. 19 where the asynchronous frequency components were filtered.

The Mho characteristic of the relay is presented in a tridimensional space of the impedance plane using the Cosine filter to estimate the phasors of voltage and current, so the reach error of the relay could be calculated (see Fig. 18). An error in the Mho characteristic is observed during the window transition and during the fault period. The reach error in the relay at this fault event is 5.8 % during the fault period compared with the fundamental characteristic. In contrast the reach error using the proposed algorithm is 0.09% (Fig. 19).

6. Summary of results

The time of fault detection of digital distance relays in operation in the power system are approximately 2-4 cycles, this is due to the transient response of the signals during the fault period, even if the algorithm restriction is 1-2 cycles [19], so the error in the operation time is evaluated during the first cycle during the fault period. This means that the results of the reduction of the error in the operation time using the proposed algorithm represent a good result, because the fault detection is performed in a time less than one cycle for the simulated case (see Table 4). Also the error compensation in the apparent impedance estimation is done during the fault period (see Table 5). Using the proposed algorithm can prevent a malfunction of the distance relay.

7. Conclusions

During a fault condition in the transmission line where the electric input signals (voltage and current) are contaminated with frequency components as interharmonics and/or subharmonics, an error in the apparent impedance estimation due to the conventional digital filtering technique will compromise the performance of the distance relay. It has been shown that the distance relay proposed algorithm causes a reach error reduction in the relay and in consequence an operation time reduction. The proposed algorithm showed good results during the fault period and the estimation times considering one cycle data window are acceptable, the estimation time is obtained by measuring the algorithm execution time in Matlab. Thus the asynchronous frequency components of voltage and current signals are identified and filtered, as a result the performance of the distance relay is enhanced.

8. Acknowledgment

The authors gratefully acknowledge the contribution of the recorded signals to Gerardo Robledo of CFE (Comisión Federal de Electricidad), México.

9. References

[1] Sigfried Heier, Grid Integration of Wind Energy Conversion Systems, second ed., Wiley, 2006.

[2] A.K. Pradhan, Joós, Adaptive distance relay setting for lines connecting wind farms, IEEE Transactions on Energy Conversion, (2007) 206-213.

[3] A. Perdana, O. Carlson, Dynamic response of grid- connected wind turbine with doubly fed induction generator during disturbances, Nordic workshop on power and industrial electronics, TRONDHEIM (2004).

[4] Nattapong Chayawatto, Egon Ortojohann, Dynamic behavior of a doubly fed induction machine with generator side converter under abnormal condition, National Science and Technology Development Agency (NSTDA), Thailand.

[5] Richard Gagnon, Gilbert Sybille, Modelling and real-time simulation of a DFIG driven by a wind turbine, IPST (2005) 162.

[6] Testa, A, Interharmonics: Theory and modeling, IEEE Transactions on Power Delivery, (2007) 2335-2348.

[7] T. Lobos, J. Rezmer, P. Schegner, Parameter Estimation of Distorted Signals, IEEE Bologna, Power Tech Conference Proceedings, (2004) 1-5.

[8] Gesche Krause, From Turbine to Wind Farms - Technical Requirements and Spin Off Products, first ed., InTech, 2011, Croatia, pp. 135-160.

[9] Sachin Srivastava, U.J. Shenoy, Abhinna Chandra Biswal and Ganesan Sethuraman, Impedance seen by Distance Relays on Lines Fed from Fixed Speed Wind Turbines, International Journal of Emerging Electric Power Systems, (2013) 17–24.

[10] Lina He, Chen-Ching Liu, Impact of LVRT Capability of Wind Turbines on Distance Protection of AC Grids, IEEE PES Innovative Smart Grid Technologies (ISGT), (2013) 1-6.

[11] Simon De Rijcke, Paula Souto Pérez and Johan Driesen, Impact of Wind Turbines Equipped with Doubly-Fed Induction Generators on Distance Relaying, IEEE Power and Energy Society General Meeting, (2010) 1-6.

[12] E.O. Schweitzer, III Schweitzer Eng. Lab., Inc., Pullman, WA, USA , D. Hou, Filtering for protective relays, WESCANEX 93. Communications, Computers and Power in the Modern Environment Conference Proceedings, IEEE, (1993) 15-23.

[13] Lennart Ljung, Modeling of Dynamic Systems, first ed., Prentice Hall, 1994.

[14] Florin Iov, Anca Daniela Hansen, Poul Sorensen, Nicolas Antonio C., Mapping of grid faults and grid codes, Riso National Laboratory, Technical University of Denmark, Roskilde Denmark, (2007).

[15] Slavomir Seman, Jouko Niiranen, Ride through analysis of doubly fed induction wind power generator under unsymmetrical network disturbances, IEEE Transactions on Power Systems, (2006) 1782-1789.

[16] IEEE Guide for Protective Relay Applications to Transmission Lines, IEEE Standard C37.113-1999, (2002).

[17] Emilson Pereira Leite, Matlab - Modelling, Programming and Simulations, first ed., Sciyo, 2010, pp 171-192.

[18] V. Cook, Analysis of Distance Protection, first ed., John Wiley & Sons, 1985.

[19] A.G. Phadke, J.S. Thorp, Computer Relaying for Power Systems, Research Studies Press LTD, Second ed., Wiley, 2009.

[20] Proakis, John G. & Manolakis, D.G. , Digital Signal Processing, fourth ed., Prentice hall, 2006.

[21] Zbigniew Leonowicz, Parametric methods for time–frequency analysis of electric signals, Politechnika Wrocławska, Wroclaw University of Technology, Poland, (2006).

[22] Li Qi, Lewei Qian, Stephen Woodruff, David Cartes, Prony Analysis for Power System Transients, EURASIP Journal on Advances in Signal Processing, (2007) 1-12.

[23] Michel Meunier, Francoise Brouaye, Fourier transform, Wavelets, Prony Analysis: Tools for Harmonics and Quality of Power, 8th International Conference on Harmonics and Quality of Power ICHQP '98, (1998) 71-76.

[24] J. F. Hauer, C.J. Demeure, L.L. Scharf, Initial results in prony analysis of power system response signals, IEEE Transactions on Power Systems, (1990) 80-89.

[25] A. R. Van C. Warrington, Protective Relays Their Theory and Practice, first ed., Springer, 1978.

[26] Gerhard Ziegler, Numerical Distance Protection Principles and Applications, third ed., Siemens AG, Wiley, 2008.

[27] Z. Lubosny, Wind Turbine Operation in Electric Power Systems, first ed., Springer, 2003.

[28] Thomas Ackerman, Wind Power in Power Systems, second ed., Wiley, 2005.

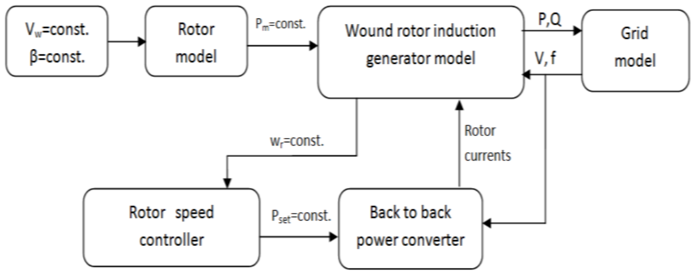

Fig. 1. Proposed model structure of DFIG scheme for analysis of operation of distance relays.

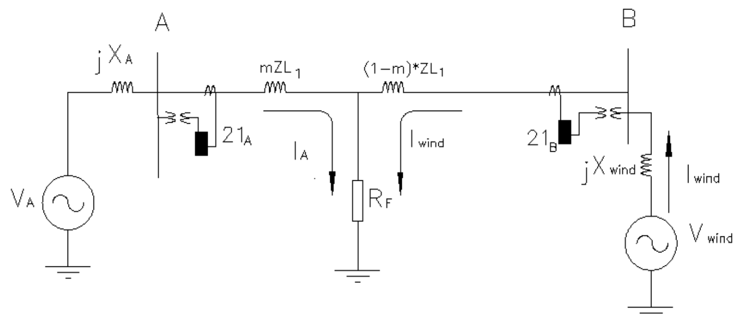

Fig. 2. One-line diagram of the test system.

Table 1
System Parameters

Test System Parameters	Values
Source A Reactance	jXA=35 Ω
Source wind power plant reactance	jXwind=6*27.54 Ω
Active power generation of wind power plant	Pwind=9MW
Transmission system voltage level	V=120kV/_0°
Line impedance ZL1	ZL1=82.4/_73.7° Ω
Fault Resistance	Rf=2 Ω
Wind speed	V_w=15m/s

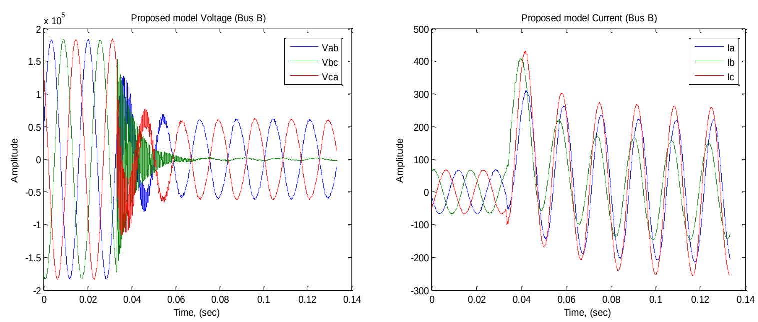

Fig. 3. Voltage and current signals of bus B for a two phase fault on the transmission line.

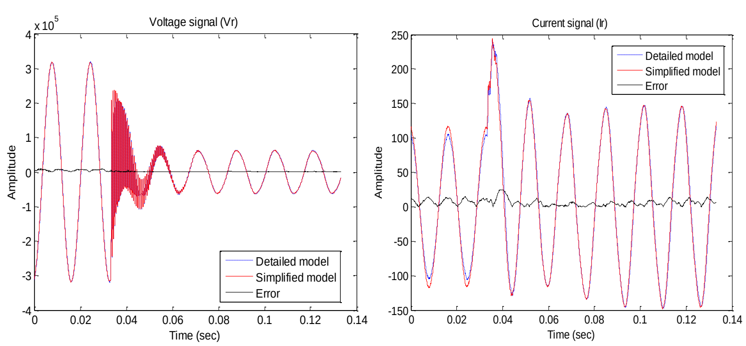

Fig. 4. Voltage and current signals at bus B for the phase relay unit (proposed and detailed model).

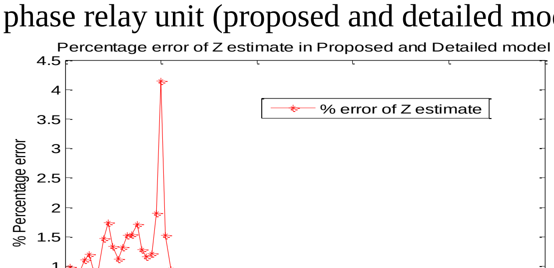

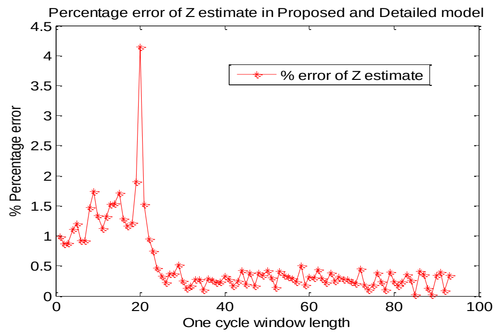

Fig. 5. Percentage error in the proposed and detailed model.

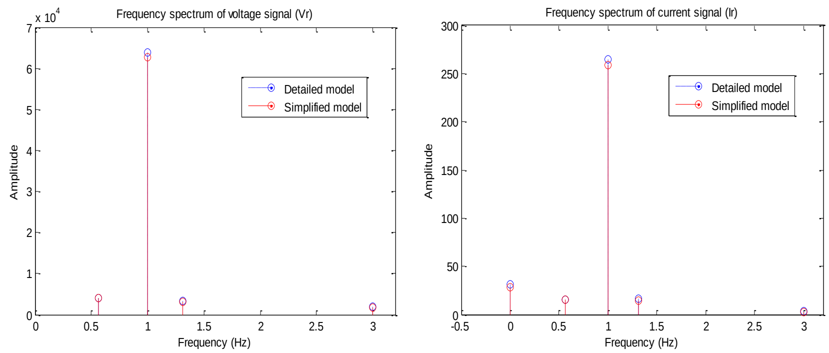

Fig. 6. Frequency spectrum of voltage (V_r) and current (I_r) signals at bus B.

Table 2
Dominant Frequencies of Voltage Signal (Detailed and Simplified model)

Frequency (Hz)	Harmonic Order	Detailed model Amplitude	Simplified model Amplitude
60.00	1.00	63770.00	60736.33
33.75	0.56	4162.00	3968.8
78.75	1.31	3377.00	3213.19
180.00	3.00	1856.00	1764.61

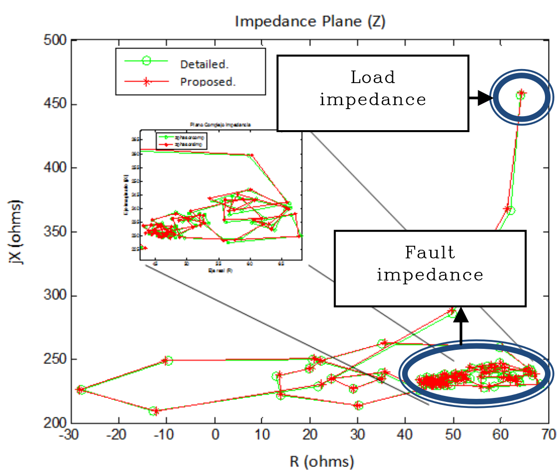

Fig. 7. Apparent impedance measurement of distance relay at bus B (detailed and proposed model).

Table 3
Dominant Frequencies of Current Signal (Detailed and Simplified model)

Frequency (Hz)	Harmonic Order	Detailed model Amplitude	Simplified model Amplitude
60.00	1.00	264.9	251.28
0.00	0.00	31.24	28.75
33.75	0.56	15.17	15.44
78.75	1.31	16.00	14.23
180.00	3.00	3.64	2.46

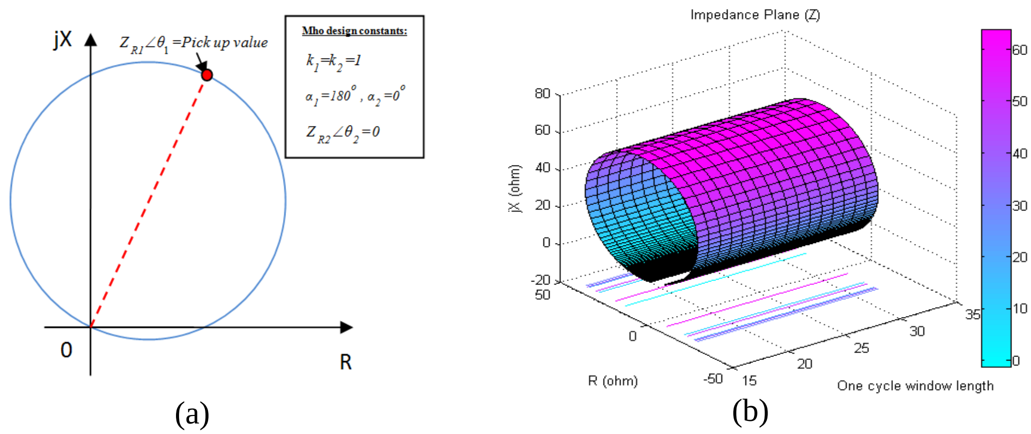

Fig. 8. Mho operation characteristic (Fundamental frequency 60Hz). a) 2D. b) 3D.

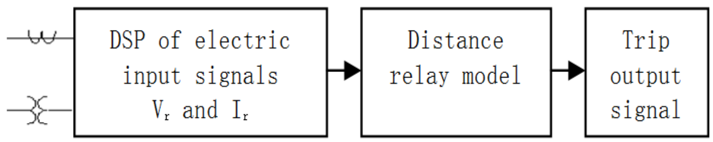

Fig. 9. Distance relay structure for input signals processing.

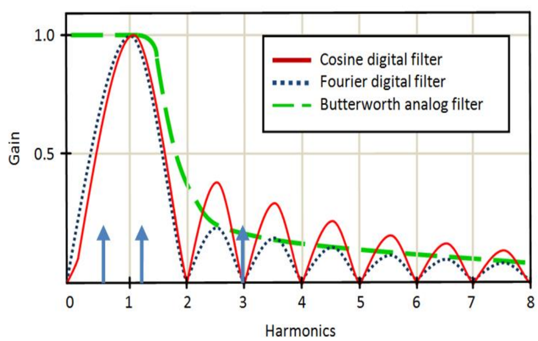

Fig. 10. Analog and digital filter frequency response used in distance relays.

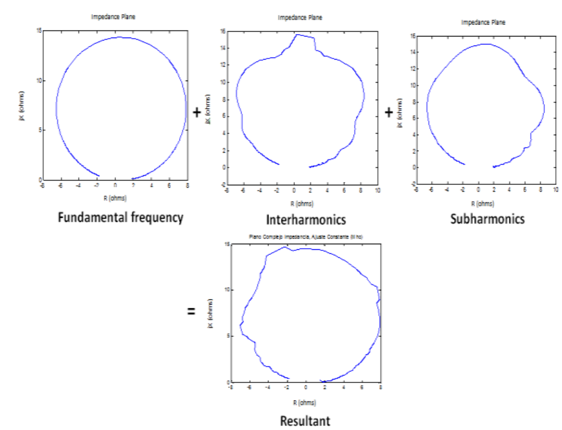

Fig. 11. Graphical representation of the error in apparent impedance estimation using digital filters.

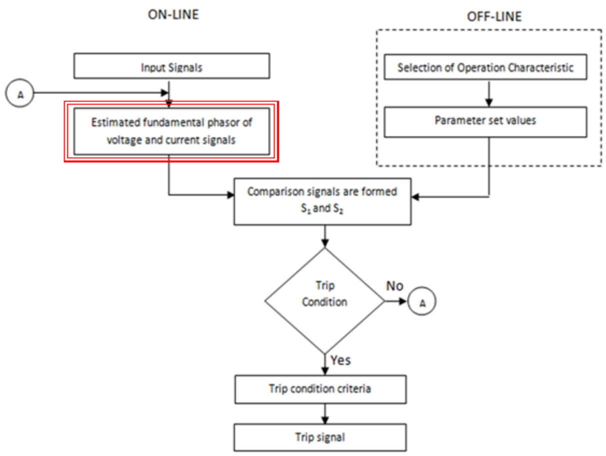

Fig. 12. Operation scheme of a distance relay model.

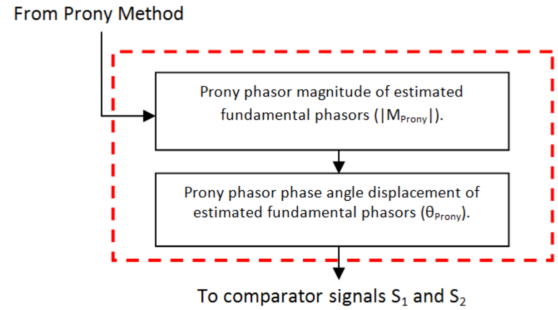

Fig. 14. Proposed distance relay algorithm using Prony method.

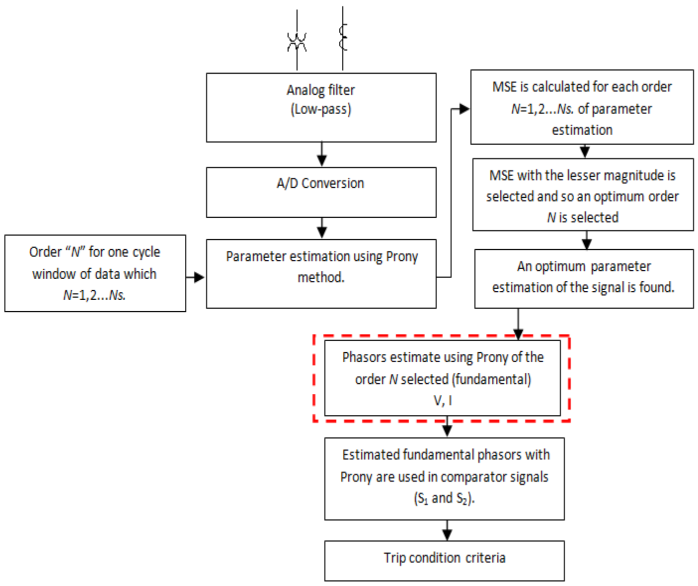

Fig. 13. Proposed distance relay algorithm using Prony method.

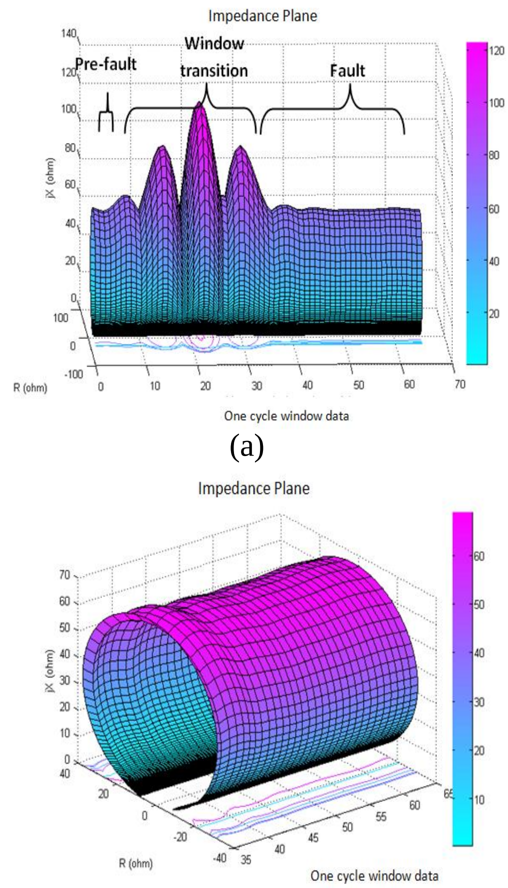

(a)

(b)

Fig. 15. Operation characteristic of a Mho distance relay at bus B. a) Side view indicating transition stages. b) Fault period.

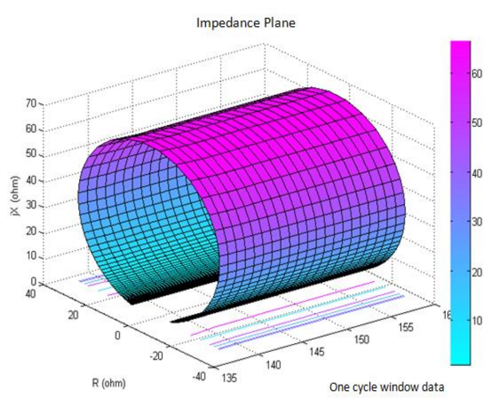

Fig. 16. Compensated Mho operation characteristic fault period (Simulated case).

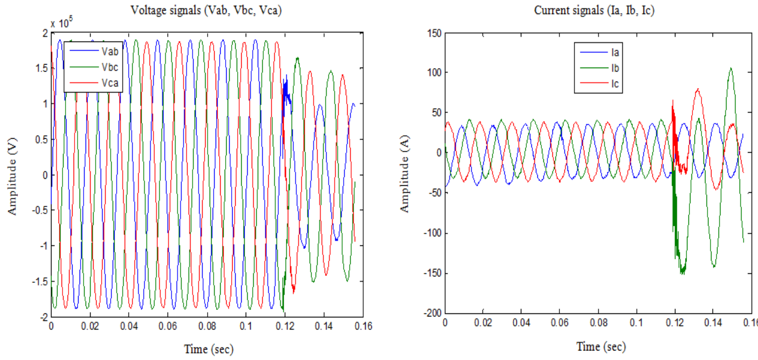

Fig. 17 Recorded fault event (voltage and current signals).

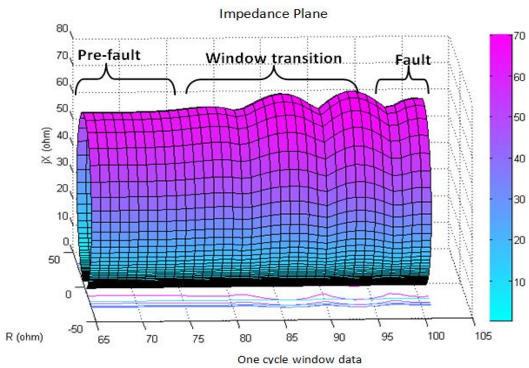

(a)

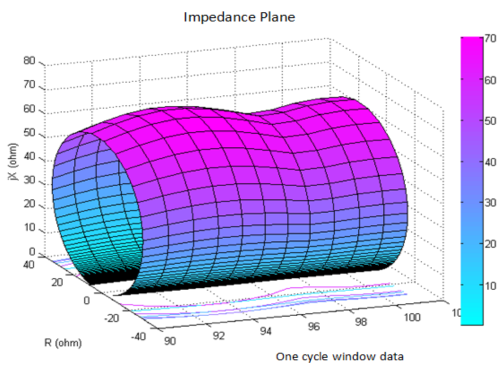

(b)

Fig. 18. Mho operation characteristic (Fault event). a) Side view indicating transition stages. b) Fault period.

Table 4
Fault detection operation time of distance relay algorithms

Simulated case	Operation time (cycles)
Cosine filter	Could not operate
Proposed algorithm	0.75

Table 5
Reach error of distance relay algorithms

Event	% Reach error (Cosine filter)	% Compensated reach error (Proposed distance relay algorithm)
Simulated case	5.7	0.02
Real fault event	5.8	0.09

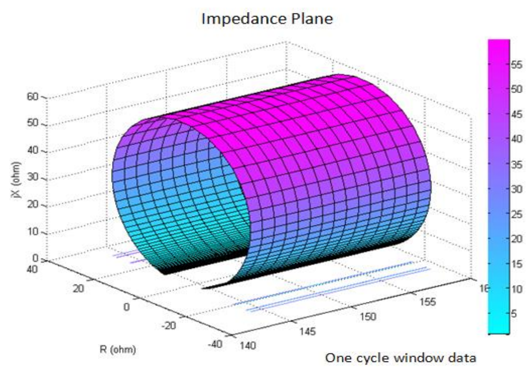

Fig. 19. Compensated Mho operation characteristic fault period (Real fault event).